HYDRODYNAMICAL CHARACTERIZATION OF RED BLOOD CELLS INTERACTIONS IN A HIGH CONFINEMENT REGIME. A COMPUTATIONAL STUDY

CARACTERIZACIÓN DE LA INTERACCIÓN HIDRODINÁMICA DE LOS GLÓBULOS ROJOS DE LA SANGRE EN RÉGIMEN DE ALTO CONFINAMIENTO. UN ESTUDIO COMPUTACIONAL

E. Navas-Conyedo[a†], Y. Costa-Marrero[b] and J. Gulín-González[a]

a) Centro de Estudio de Matemática Computacional (CEMC), Grupo de Matemática y Física Computacionales, Facultad de Ciencias y Tecnologías Computacionales, Universidad de las Ciencias Informáticas (UCI), 19370 La Habana, Cuba; enavas@uci.cu†
b) Departamento de Ciencias Básicas, Facultad 3, UCI, 19370 La Habana, Cuba
† corresponding author

Recibido 16/3/2017; Aceptado 25/10/2017

The red blood cells (RBCs) have a critical role in order to understand the properties of blood in a high confinement regime. Thus, the ability of RBCs to change the shape allows them to flowing through small microcapillaries in the order of $10\,\mu m$ of diameter, according to the membrane viscoelastic properties, with a complex non-linear blood flow behavior. In the previously mentioned conditions it is very important to take into account that the inter-cells hydrodynamical interaction can be critically important in order to consider the effect of solvent media like an indirect interaction transmission media. In the bibliography consulted were shown the dependence of the confinement and the flow ratio on the RBC's shape and on the length of perturbation in the surrounding flow for the case of single vesicle simulation, but the effects of closed RBCs and it dynamics behavior were omitted. In the present paper, we use the length of perturbation as a critical parameter to estimate the hydrodynamics interacting range. Subsequently, simulations in a system with two RBCs were used to study the inter-cells hydrodynamic interaction, a two-dimensional reduced model is used. The RBC was modeled as a vesicle formed by a ring of interacting particles. The solvent-solvent and solvent-RBC particles interactions were computed by Multiparticle Collision Dynamics mesoscale computational technique. Here we propose a general hydrodynamic interaction model description including the relative cell-cell distance, velocity, flow and confinement regime. As result of simulations a stochastic exponential decay hydrodynamic force was observed, when the cell-cell distance is near to the double of lengths of perturbation.

Las células de glóbulos rojos de la sangre (RBCs) cumplen un papel decisivo en el entendimiento de las propiedades de la sangre en régimen de alto confinamiento. La capacidad de los RBCs de cambiar de forma les posibilita el paso a través de pequeños microcapilares en el orden de $10\,\mu m$ de diámetro , lo cual depende de las propiedades viscoelásticas de la membrana celular, y se manifiesta en un comportamiento no-lineal del microfluido. En las condiciones mencionadas anteriormente es necesario tener en cuenta que las interacciones hidrodinámicas entre las células juegan un rol relevante, considerando además que el solvente constituye el medio indirecto de propagación de esta interacción. En las bibliografía consultada se muestra la dependencia de la forma de un RBCs y la distancia de perturbación en el fluido circundante en función del confinamiento y el flujo, pero se omiten los efectos de RBCs cercanos y sus dinámicas. En el presente artículo utilizamos la distancia de perturbación en el fluido circundante como parámetro crítico en la estimación del rango de las interacciones hidrodinámicas entre RBCs . Además, simulaciones de dos RBCs son utilizadas para analizar las características de la interacción hidrodinámica entre las células, a partir de la cuál se propone un modelo de interacción hidrodinámico dependiente de la distancia entre células, la velocidad relativa y el confinamiento del fluido utilizando un modelo bidimensional. Los RBCs son modelados como vesículas en forma de anillos de partículas interactuantes. La interacción entre las partículas del solvente y de estas con las partículas de los RBCs es modelado por la técnica mesoscópica de Colisiones de Múltiples Partículas. Se propone un modelo general de seudo-fuerza de interacción hidrodinámica, con características estocástica y decrecimiento exponencial con la distancia cuando esta está en el orden del doble de la distancia de perturbación en el fluido circundante.

PACS: Flow computation, 47.11.-j; Computational techniques mathematics, 02.70.-c; Capillary effects (interfacial flows), 47.55.nb

I. INTRODUCTION

The behavior of blood fluid in microcapillaries is governed by the red blood cells properties (RBC). In general, the main factors that influence the blood fluid behavior are the hematocrits degree or RBCs concentration, the plasma viscosity, RBCs aggregation and deformability as well as elastic-geometric characteristics of channel vessels, arteries or microcapillaries. However, in high confinement regime with a low flow Reynold number and capillaries in order of sizes of $10\,\mu m$ (near to the effective RBCs size), the principal factor is the RBC deformability with a non-Newtonian behavior [1–3]. The most important mechanical RBC factor is the membrane properties, due to their influence in the ability of RBC to adapt their shape according to the flow, it is known that the alteration of RBCs viscoelastic properties are related with various pathologies [4]. The RBC geometric shape affects the microscopic distribution of oxygen tension

and the hemoglobin saturation, the increment of the RBC deformation makes the flow more uniform near to the walls and the oxygen flux decrease, this effect is balanced by the circulation of RBCs [5].

Morphologically RBC membrane is formed by a phospholipid bilayer, with a bending and expansion moduli, and an underlying spectrin network cytoskeleton which prevent the large membrane deformation producing a large elastic shear modulus. Some approaches have been proposed to deal with membrane complex structure and behavior [6], one of the most used methods is to represent a membrane as a network of mesoscopic particles connected, and incorporate this structure into a dynamic formalism like Multiparticle Collision Dynamics (MPC, also known as Stochastic Rotation Dynamics) that has obtained a very detailed membrane description [1,7]. Furthermore, in some cases is possible to apply a two dimensional approach that qualitatively capture the RBC behavior and enable more extensible sweep of capillary number avoiding the constraints of the computational time for three-dimensional domain, essentially the neo-Hookean and Mooney-Rivlin models for strain energy and tension can be applied to dimension reduction [6]. This have enormous advantages and in fact reproduce many of experimental and theoretical results.

The simulation of blood microfluids requires the use of coarse-grained approaches for reproducing the behavior of complicated structures with the essential features of physics models, such as MPC [8]. The MPC mesoscopic method is the less complicated computational method where the solvent is modeled as particle gas that performs two steps: a streaming step and the collision step. The complex structures, like RBC membrane, are modeled with molecular dynamics and the solvent-complex structures interaction are modeled in the MPC collision step. During the streaming step the solvent particles are moved as an ideal gas with external interactions. When the collision step is performed all particles in the system are sorted in regular boxes and the velocities of particles are changed according to a rule that guaranties some conservation laws like energy and linear momentum. MPC defines a discrete-time hydrodynamics which has been shown to yield correct hydrodynamic behavior at long enough times, and can be applied to equilibrium and non-equilibrium fluid studies. A more complete description of MPC method can be found in references [9–12].

In high confinement regime RBCs are aligned in a single row and their dynamics are dominated by the interactions with the walls rather than neighboring RBCs. Moreover, if the concentration increases the collective effects substantially changes the flow properties with a rapidly viscosity change by the formation of a cell layer near to the walls, the flow induce a vesicles migration to the center of channel and the existence of a cell depleted region near walls, here deformability has a main role [2,13]. In these conditions the RBCs movements are correlated and in correspondence with the flow rate with a tendency from independent movement to high correlate movement as a single file [7,14], this behavior suggests that a one dimensional dynamics treatment could be applied.

Any RBC has an influence in the surrounding flow with a perturbation over the flow profile, which rapidly decay far away. That suggests the existence of an interaction via solvent media between RBCs. In this work we establish a relation between the penetration length defined for a single RBC in a two dimensional Poiseuille flow with inter-cells hydrodynamic interaction as a stochastic exponential decay hydrodynamic force. Furthermore, a dynamic description using Langevin equation was compared with simulations results when the mean distance between RBCs is in order to the double of penetration length.

The proposed stochastic interactions model allow the extension of results for describing large systems, when non-linear effects are relevant without large RBCs shape changes.

II. MATERIALS AND METHODS

During the simulations the flow behavior was described by the MPC steps. During the streaming step the positions and velocities are updated using velocity-Verlet method, including periodical boundary condition in x-axes for enough length $L \gg R_{RBC}$, where R_{RBC} is the effective RBC radii, furthermore, the bounce-back rule with ghost y-wall particles rule is used [15,16]. In MPC the solvent is considered as an ideal gas of particles where only external interactions, i.e gravity to drive fluid movement, are considered in the stream step. In the collision step all particles are sorted into N homogeneous boxes of length a, the boxes origin of coordinates are randomly changed on every iteration to provide galilean invariance as $x_i = (N_i + 0.5\xi_i)$, where N_i is the discretization number and ξ_i is a uniform random number in $[-1, 1]$ interval on each i-axes [8].

We select the the MPC-AT-a variant which provides an implicit Andersen thermostat, for including the thermals fluctuation. In the collision step on each box the particles velocity were updated as follows:

$$\vec{V}_i^{*} = \vec{V}_{CM} + \vec{V}^i_{rand} - \frac{\sum m_i \vec{V}^i_{rand}}{\sum m_i}$$

where $\vec{V}^i_{rand}$ is a random velocity generated with Maxwell-Boltzmann distribution at temperature T, $\vec{V}_{CM}$ is the box center mass velocity and m_i is the mass of each box particle [9]. The coupling between solvent and complex structures was done during the collision step, on which all particles participate.

The RBC membrane was described by a discrete spring ring of N_{RBC} particles which interacts by elastic (1) and bending (2) interactions potential energies. A surface constraint potential energy was also included for modeling the RBC incompressibility (3).

$$U^i_k = K_s \left(\frac{(l_i^3 + 2)}{l_i} - 3 \right) \tag{1}$$

$$U^i_B = K_{Ben}(1 - \frac{\vec{r}_{i-1,i} \bullet \vec{r}_{i,i+1}}{r_{i-1,i}\, r_{i,i+1}}) \tag{2}$$

$$U_A = K_A(\frac{A}{A_0} - 1)^2 \tag{3}$$

The elastic interaction between neighbor spring particles is described by equation (1), where K_s is the Mooney-Rivlin elastics constant, $l_i = r_{i,i+1}/ro$, with r_0 a constant that defines the desired total membrane arclength $L_{RBC} = N_{RBC} r_0$ and $r_{i,i+1}$ is the distance between neighbor spring particles [17]. The bending interaction is described by equation (2) with K_{Ben} strength constant. In the equation (3) K_A is surface constant constrain, A_0 is the desired RBC surface and A is the measured surface. For maintaining the relation between the RBC surface and arclength, K_A must be selected with enough large value [3].

We introduce Morse modified repulsive potential to avoid RBCs overlapping:

$$U_{rep}^{A,B} = K_B T \left(Exp\left(\frac{2\,(s_0 - r_{A,B})}{s_0} \right) - \frac{r_{A,B}}{s_0} \right) \; r_{A,B} \leq s_0 \tag{4}$$

where $s_0 \sim 2\,r_0$.

If is consider the theoretical Naiver-Stokes velocity profile $V_f^0(y) = \frac{\rho\, g_r\, y(W-y)}{2\,\eta}$ for a two dimensional Poiseuille flow for W channel width ρ solvent density and η solvent viscosity with the action of uniform gravity g_r, moreover the difference amplitude of perturbed profile, measured from single RBC center, as:

$$R(x) = \int_0^W \left| V(x,y) - V_f^0(y) \right| dy$$

the penetration length l_p can be obtained by fitting to $R(x) = R_0 exp\left(-\left(\frac{x}{l_p} \right)^2 \right) + R_G$, where R_0 is the amplitude and R_G the background noise [18].

To characterize the single RBC state, the flow dimensionless flow strength over vesicle deformation C_k and the RBC confinement C_n were used as follows:

$$C_k = \frac{\eta \dot{\gamma}_w R^3}{\kappa} \tag{5}$$

$$C_n = \frac{2R}{W} \tag{6}$$

where, $\kappa \sim 4\,K_{Ben}$ is the bending rigidity, $R = \sqrt{A_0/\pi}$, and $\dot{\gamma}_w = \frac{\partial V_x}{\partial y}|_w = \frac{\rho\, g_r\, W}{2\,\eta}$ is the value of wall velocity shear rate for only solvent Poiseuille flow. These states are used to describe the stable shapes and penetration length according to the RBCs and flow properties [1, 19].

The high confinement regime can be understood as $C_n > 0.6$, and normal values for C_k are in the range $\{0.5, 15.0\}$ [20]. It is known that for a selected parameters pair C_k and C_n. the RBCs has a corresponding shape, for this reason we make the studies for a confinement of 0.9 where the shape changes are smooth and they do not move overlapping.

III. RESULTS AND DISCUSSION

The setup system is corresponding with a 2D Poiseuille flow in x-axes for a confinement of 0.9. The configuration have a x-length $L = 100\ a$, y-width $W = 2\sqrt{A_0/\pi}/C_n \approx 13\ a$, the number of solvent particles in $N = n_c LW = 13000$, 1300 MPC boxes and 100 ring membrane particles per RBC of mass $m_v = 10\ M_s$. The selected parameters are show in table I, which corresponds to values used for similar conditions in references [2, 21–23].

Table 1. Dimensionless parameter using in simulations

Parameter/Description	Value
ρ Solvent density	$n_C = 10$ (real 1000 $K_g\ m^{-3}$)
a Box Length	1 (real $1\mu\ m$)
L System Length	100
M_s Solvent particle mass	1
$K_B T(35^0 C)$ Thermal energy	1
t_0 Time unit	1
η_0 Viscosity unit	1
η Solvent viscosity	1396.6 (real 1.2 $10^{-3} Pas$)
t_{MPC} Time step	0.000537023
K_{Ben}RBC Bending constant	26.181
K_s RBC MR elastics constant	70286
L_{RBC} RBC 2D arclength	46.1373
K_A RBC Surface contant	10^7
A_0 RBC 2D cross surface	105.645
A^* RBC reduced area	0.623668

Initially we estimate the penetration length according to C_k flow parameter using the simulations of a single RBC, which are showed in figure 1 a). As was refer in [18] the penetration length has a tendency to exponentially decay as C_k increases to the maximum length from the membrane to the RBCs center mass, as well as the shape tends to parachute form. In the figure 1 b) it is shown the mean value of the esphericity $\alpha = \frac{(\lambda_+ - \lambda_-)^2}{(\lambda_+ + \lambda_-)^2}$, which is a magnitude of reference of the shape, where $\{\lambda_-, \lambda_+\}$ are the low and major eigenvalues of the inertia tensor. For values near to 0.2 the shape is a discoid and for 0.1 is parachute.

For two RBCs at different relative x-distances $L_0 \in \{1.9, 2.0, 2.5, 3.0, 4.0\}\, L_p$ at the beginning of simulation, the relative velocity variance is measured for flow in $C_k \in \{5.0, 10.0\, 15.0\}$ and shown in Figure 2 (a), according to the simulation parameters and time scales the relative distance does not change significantly, this allows to measure the local dynamics, which is showed in Figure 2 (b) this corresponds to a high speed regime. From Figure 2 (a) we observed a tendency for coupling movement when the RBCs are near each other with strong correlation, as the relative distance increases the movement is independent with thermal fluctuations coupled with the flowing *(blue line)* [24].

We propose a one-dimensional Langevin based dynamic stochastic model according to equations (III) for describing the previous showed results, where X_i is the position of each RBCs center mass, X_{ij} is the relative RBCs center

mass position, M_i the mass for each RBC, $\gamma = \frac{M_i g_r}{<\dot{X}_i>}$ the effective friction coefficient for a $< \dot{X}_i >$ mean velocity, W^G is uncorrelated Gaussian noise with zero mean and unit variance, and $K_B T$ the thermal energy, η_S is the membrane viscosity and η_M is the solvent viscosity.

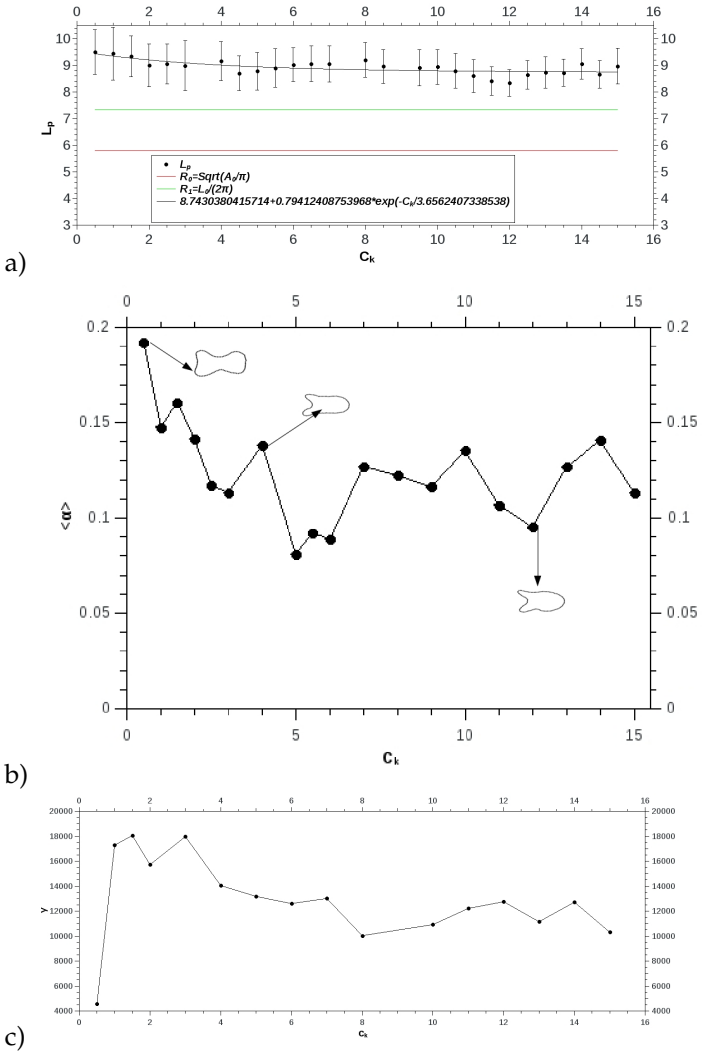

Figure 1. a) Penetration length for $C_n = 0.9$ and $C_k \in (0.5, 15.0)$, R_0 the radii of a circle of the same area and $R_1$the radii of a circle of the same arclength is showed for comparison. The results are fitting to a exponential decay law as is recommended in Ref [18]. b) Esphericity versus C_k values, a tendency from discoid to parachute is observed. c) Effective friction coefficient γ, the non-linear effects acording to the RBC shape are observed

The values of γ and L_p were obtained from single RBC simulation, Figure 2 a) and c), which depends of selected C_K and C_n setup, and included in the theoretical result shown in Figure 2 (a) *(theoretical lines)*. In our case the value of $C_n = 0.9$ was fixed and the obtained parameters have an non-linear explicit dependence with the flow gravity g_r (i.e. C_K) according to (5) described before.

The flow profile in the y-axes has a flat form near to the region occupied by the RBC, which variate with the hydrodynamic shape figure:1 (b) according to the setup, because of this the momentum interchange between the RBC,walls and flow has a marked non-linear effect [25], which is expressed in γ values. This model has some similarities with DPD simulation technique, essentially the weight function U adjusted to reproduce the variance tendency is different [26].

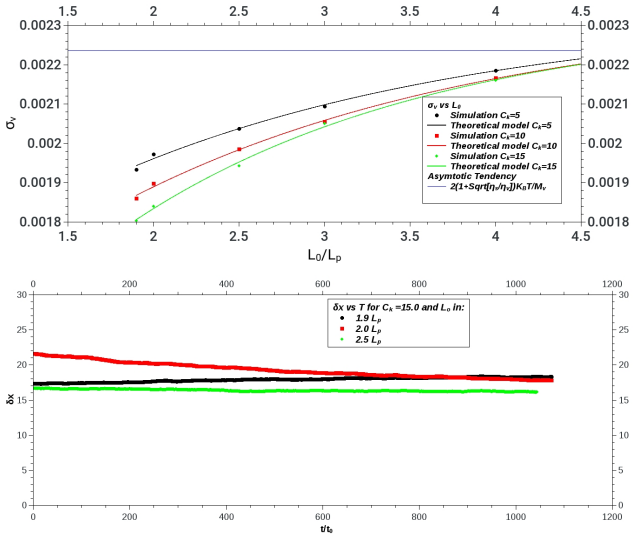

Figure 2. a) Relative velocity variance for two RBCs at different initial distances from simulation and theoretical model from equation (III). b) Relative distance between RBCs for $C_k = 15.0$ and initial distance in $\{1.9, 2.0, 2.5\}\, L_p$.

These behavior can be interpreted as a relative distance dependence of fluctuation-dissipation relation, moreover this reveals that if the distances between RBCs are large enough, the hydrodynamic perturbation field is not overlapped and independent movement can be consider. Thus, if the RBCs are very closed the cell-cell interactions are strong with extra non-linear effects, and the proposed dynamic model may be not applied.

$$M_i \ddot{X}_i = M_i g_r - \gamma \dot{X}_i + \sqrt{2\gamma K_B T} W_i^G(t) + \sum_{j \neq i} F_{ji}^S(X_{ji}, \dot{X}_{ji}, t) \qquad (7)$$

$$F_{ji}^S(X_{ji}, \dot{X}_{ji}, t) = -\sqrt{\frac{\eta_S}{\eta_M}} \gamma U(X_{ji}) \dot{X}_{ji} + \sqrt{2\, U(X_{ji})\, \gamma \sqrt{\frac{\eta_S}{\eta_M}}\, K_B T} W_{ji}^G(t) \qquad (8)$$

$$U(X_{ji}) = 1 - Exp\left(\frac{-|X_{ji}|}{2 L_p}\right) \qquad (9)$$

IV. CONCLUSIONS

The penetration length contains significant information of the impact of each RBCs in flow conditions, it can be used to cell-cell hydrodynamic interactions description. This information can be used in conditions in which the RBCs shapes have not significant changes and the confinement allow the application of one-dimensional stochastic interaction model as we propose in equation (III). This model showed a good agreement with the simulations, and the cell-cell dynamical behavior was adequately reproduced in RBCs.

Furthermore, the results can be extended for the case of many RBCs in a narrow flow channel, with the possibility to analyze the evolution of the density of a system as a Langevin processes in large coordinate spaces and then using projection operator techniques to obtain a hierarchy of equations for the n point density correlation functions which was reported in [27].

ACKNOWLEDGMENT

Thank to ICS-2/IAS-2 Forchungszentrum Jülich, Alexander von Humboldt Foundation and Universidad de las Ciencias Informáticas of La Havana, Cuba, for the financial support of this research.

REFERENCES

[1] G. R. Lazaro, A. Hernandez-Machado and I. Pagonabarraga, Soft Matter **10**, 7195 (2014).
[2] P. Bagchi, Biophys. J. **92**, 1858 (2007).
[3] S. Chien, Annu. Rev. Physiol. **49**, 177 (1987).
[4] G. Prado, A. Farutin, C. Misbah and L. Bureau, Biophys. J. **108**, 2126 (2015).
[5] C. H.Wang and A. S. Popel, Math. Biosci. **116**, 89 (1993).
[6] D. Barthes-Biesel, A. Diaz and E. Dhenin, J. Fluid Mech. **460**, 211 (2002).
[7] D. A. Fedosov, M. Peltomaki and G. Gompper, Soft Matter **10**, 4258 (2014).
[8] K. Tucci and R. Kapral, J. Phys. Chem. B **109**, 21300 (2005).
[9] H. Noguchi, N. Kikuchi and G. Gompper, EPL **78**, 10005 (2007).
[10] I. O. Götze, H. Noguchi and G. Gompper, Phys. Rev. E **76**, 046705 (2007).
[11] S. Poblete, A.Wysocki, G. Gompper and R. G.Winkler, Phys. Rev. E **90**, 033314 (2014).
[12] E. Westphal, S. Singh, C.-C. Huang, G. Gompper and R. Winkler, Comput. Phys. Commun. **185**, 495 (2014).
[13] P. M. Vlahovska, T. Podgorski and C. Misbah, Comptes Rendus Physique **10**, 775 (2009).
[14] J. Sane, J. T. Padding and A. A. Louis, Faraday Discuss. **144**, 285 (2010).
[15] I. Rao and K.Rajagopal, Acta Mechanica **135**, 113 (1999).
[16] H. Zhao and E. S. G. Shaqfeh, Phys. Rev. E **83**, 061924 (2011).
[17] S. Ye, Y. Ng, J. Tan, H. Leo and S. Kim, Theor. Biol. Med. Modell. **11**, 19 (2014).
[18] G. R. Lazaro, Red blood cell mechanics: from membrane elasticity to blood rheology, PhD thesis, Universitat de Barcelona (2014).
[19] B. Kaoui, N. Tahiri, T. Biben, H. Ez-Zahraouy, A. Benyoussef, G. Biros and C. Misbah, Phys. Rev. E **84**, 041906 (2011).
[20] G. R. Lazaro, A. Hernandez-Machado and I. Pagonabarraga, Soft Matter **10**, 7207 (2014).
[21] D. A. Fedosov, B. Caswell and G. E. Karniadakis, Comput. Methods Appl. Mech. Eng. **199**, 1937 (2010).
[22] M. Navidbakhsh and M. Rezazadeh, Scientia Iranica B **19**, 1329 (2012).
[23] H. Aminikhah and A. Jamalian, Scientia Iranica B **19**, 1133 (2012).
[24] P. Bagchi, P. C. Johnson and A. S. Popel, J. Biomech. Eng. **127**, 1070 (2005).
[25] D. Katanov, G. Gompper and D. A. Fedosov, Microvasc. Res. **99**, 57 (2015).
[26] M. K. Petersen, J. B. Lechman, S. J. Plimpton, G. S. Grest, P. J. Veld and P. R. Schunk, J. Chem. Phys. **132**, 174106 (2010).
[27] D. S. Dean, J. Phys. A: Math. Gen. **29**, L613 (1996).